

Search for the lepton number violation decay $\phi \rightarrow \pi^+ \pi^+ e^- e^-$ via $J/\psi \rightarrow \phi \eta^*$

M. Ablikim (麦迪娜)¹ M. N. Achasov^{4,c} P. Adlarson⁷⁵ O. Afedulidis³ X. C. Ai (艾小聪)⁸⁰ R. Aliberti³⁵
A. Amoroso^{74A,74C} M. R. An (安美儒)³⁹ Q. An (安琪)^{71,58,a} Y. Bai (白羽)⁵⁷ O. Bakina³⁶ I. Balossino^{29A}
Y. Ban (班勇)^{46,h} H.-R. Bao (包浩然)⁶³ V. Batzskaya^{1,44} K. Begzsuren³² N. Berger³⁵ M. Berlowski⁴⁴
M. Bertani^{28A} D. Bettoni^{29A} F. Bianchi^{74A,74C} E. Bianco^{74A,74C} A. Bortone^{74A,74C} I. Boyko³⁶ R. A. Briere⁵
A. Brueggemann⁶⁸ H. Cai (蔡浩)⁷⁶ X. Cai (蔡啸)^{1,58} A. Calcaterra^{28A} G. F. Cao (曹国富)^{1,63} N. Cao (曹宁)^{1,63}
S. A. Cetin^{62A} J. F. Chang (常劲帆)^{1,58} G. R. Che (车国荣)⁴³ Y. Z. Che (车逾之)^{1,58,63} G. Chelkov^{36,b}
C. Chen (陈琛)⁴³ Chao Chen (陈超)⁵⁵ G. Chen (陈刚)¹ H. S. Chen (陈和生)^{1,63} M. L. Chen (陈玛丽)^{1,58,63}
S. J. Chen (陈申见)⁴² S. L. Chen (陈思璐)⁴⁵ S. M. Chen (陈少敏)⁶¹ T. Chen (陈通)^{1,63} X. R. Chen (陈旭荣)^{31,63}
X. T. Chen (陈肖婷)^{1,63} Y. B. Chen (陈元柏)^{1,58} Y. Q. Chen³⁴ Z. J. Chen (陈卓俊)^{25,i} Z. Y. Chen (陈正元)^{1,63}
S. K. Choi¹⁰ G. Cibinetto^{29A} S. C. Coen³ F. Cossio^{74C} J. J. Cui (崔佳佳)⁵⁰ H. L. Dai (代洪亮)^{1,58}
J. P. Dai (代建平)⁷⁸ A. Dbeyssi¹⁸ R. E. de Boer³ D. Dedovich³⁶ Z. Y. Deng (邓子艳)¹ A. Denig³⁵ I. Denysenko³⁶
M. Destefanis^{74A,74C} F. De Mori^{74A,74C} B. Ding (丁彪)^{66,1} X. X. Ding (丁晓萱)^{46,h} Y. Ding (丁勇)⁴⁰ Y. Ding (丁逸)³⁴
J. Dong (董静)^{1,58} L. Y. Dong (董燎原)^{1,63} M. Y. Dong (董明义)^{1,58,63} X. Dong (董翔)⁷⁶ M. C. Du (杜蒙川)¹
S. X. Du (杜书先)⁸⁰ Z. H. Duan (段宗欢)⁴² P. Egorov^{36,b} Y. H. Fan (范宇晗)⁴⁵ J. Fang (方建)^{1,58}
S. S. Fang (房双世)^{1,63} W. X. Fang (方文兴)¹ Y. Fang (方易)¹ Y. Q. Fang (方亚泉)^{1,58} R. Farinelli^{29A} L. Fava^{74B,74C}
F. Feldbauer³ G. Felici^{28A} C. Q. Feng (封常青)^{71,58} J. H. Feng (冯俊华)⁵⁹ K. Fischer⁶⁹ M. Fritsch³
C. D. Fu (傅成栋)¹ J. L. Fu (傅金林)⁶³ Y. W. Fu (傅亦威)^{1,63} H. Gao (高涵)⁶³ Y. N. Gao (高原宁)^{46,h}
Yang Gao (高扬)^{71,58} S. Garbolino^{74C} I. Garzia^{29A,29B} L. Ge (葛玲)⁸⁰ P. T. Ge (葛潘婷)⁷⁶ Z. W. Ge (葛振武)⁴²
C. Geng (耿聪)⁵⁹ E. M. Gersabeck⁶⁷ A. Gilman⁶⁹ K. Goetzen¹³ L. Gong (龚丽)⁴⁰ W. X. Gong (龚文焯)^{1,58}
W. Gradl³⁵ S. Gramigna^{29A,29B} M. Greco^{74A,74C} M. H. Gu (顾旻皓)^{1,58} Y. T. Gu (顾运厅)¹⁵ C. Y. Guan (关春懿)^{1,63}
A. Q. Guo (郭爱强)^{31,63} L. B. Guo (郭立波)⁴¹ M. J. Guo (国梦娇)⁵⁰ R. P. Guo (郭如盼)⁴⁹ Y. P. Guo (郭玉萍)^{12,g}
A. Guskov^{36,b} J. Gutierrez²⁷ T. T. Han (韩婷婷)¹ W. Y. Han (韩文颖)³⁹ X. Q. Hao (郝喜庆)¹⁹ F. A. Harris⁶⁵
K. K. He (何凯凯)⁵⁵ K. L. He (何康林)^{1,63} F. H. Heinsius³ C. H. Heinz³⁵ Y. K. Heng (衡月昆)^{1,58,63} C. Herold⁶⁰
T. Holtmann³ P. C. Hong (洪鹏程)^{12,g} G. Y. Hou (侯国一)^{1,63} X. T. Hou (侯贤涛)^{1,63} Y. R. Hou (侯颖锐)⁶³
Z. L. Hou (侯治龙)¹ B. Y. Hu (胡碧颖)⁵⁹ H. M. Hu (胡海明)^{1,63} J. F. Hu (胡继峰)^{56,j} T. Hu (胡涛)^{1,58,63}
Y. Hu (胡誉)¹ G. S. Huang (黄光顺)^{71,58} K. X. Huang (黄凯旋)⁵⁹ L. Q. Huang (黄麟钦)^{31,63} X. T. Huang (黄性涛)⁵⁰
Y. P. Huang (黄燕萍)¹ T. Hussain⁷³ F. Hölzken³ N. Hüsken^{27,35} N. in der Wiesche⁶⁸ J. Jackson²⁷ S. Jaeger³
S. Janchiv³² Q. Ji (纪全)¹ Q. P. Ji (姬清平)¹⁹ X. B. Ji (季晓斌)^{1,63} X. L. Ji (季筱璐)^{1,58} Y. Y. Ji (吉钰瑶)⁵⁰
X. Q. Jia (贾晓倩)⁵⁰ Z. K. Jia (贾泽坤)^{71,58} H. B. Jiang (姜候兵)⁷⁶ P. C. Jiang (蒋沛成)^{46,h} S. S. Jiang (姜赛赛)³⁹

Received 31 August 2024; Accepted 26 December 2024; Published online 27 December 2024

* The BESIII Collaboration appreciates the staff of BEPCII and the IHEP Computing Center for their strong support. This work is supported in part by the National Key R&D Program of China (2020YFA0406300, 2020YFA0406400); National Natural Science Foundation of China (NSFC) (12035009, 11635010, 11735014, 11835012, 11935015, 11935016, 11935018, 11961141012, 12025502, 12035013, 12061131003, 12192260, 12192261, 12192262, 12192263, 12192264, 12192265, 12221005, 12225509, 12235017); the Chinese Academy of Sciences (CAS) Large-Scale Scientific Facility Program; the CAS Center for Excellence in Particle Physics (CCEPP); Joint Large-Scale Scientific Facility Funds of the NSFC and CAS (U1832207); CAS Key Research Program of Frontier Sciences (QYZDJ-SSW-SLH003, QYZDJ-SSW-SLH040); 100 Talents Program of CAS; the Institute of Nuclear and Particle Physics (INPAC) and Shanghai Key Laboratory for Particle Physics and Cosmology; the European Union's Horizon 2020 research and innovation program under the Marie Skłodowska-Curie grant agreement (894790); the German Research Foundation DFG (455635585), the Collaborative Research Center CRC 1044, FOR5327, GRK 2149; Istituto Nazionale di Fisica Nucleare, Italy; Knut and Alice Wallenberg Foundation (2021.0174, 2021.0299); Ministry of Development of Turkey (DPT2006K-120470); National Research Foundation of Korea (NRF-2022R1A2C1092335); National Science and Technology Fund of Mongolia; National Science Research and Innovation Fund (NSRF) via the Program Management Unit for Human Resources & Institutional Development, Research and Innovation of Thailand (B16F640076); Polish National Science Centre (2019/35/O/ST2/02907); Swedish Research Council (2019.04595); the Swedish Foundation for International Cooperation in Research and Higher Education (CH2018-7756); and the U. S. Department of Energy (DE-FG02-05ER41374).



Content from this work may be used under the terms of the Creative Commons Attribution 3.0 licence. Any further distribution of this work must maintain attribution to the author(s) and the title of the work, journal citation and DOI. Article funded by SCOAP³ and published under licence by Chinese Physical Society and the Institute of High Energy Physics of the Chinese Academy of Sciences and the Institute of Modern Physics of the Chinese Academy of Sciences and IOP Publishing Ltd

- T. J. Jiang (蒋庭俊)¹⁶ X. S. Jiang (江晓山)^{1,58,63} Y. Jiang (蒋艺)⁶³ J. B. Jiao (焦健斌)⁵⁰ Z. Jiao (焦铮)²³
 S. Jin (金山)⁴² Y. Jin (金毅)⁶⁶ M. Q. Jing (荆茂强)^{1,63} X. M. Jing (景新媚)⁶³ T. Johansson⁷⁵ S. Kabana³³
 N. Kalantar-Nayestanaki⁶⁴ X. L. Kang (康晓琳)⁹ X. S. Kang (康晓坤)⁴⁰ M. Kavatsyuk⁶⁴ B. C. Ke (柯百谦)⁸⁰
 V. Khachatryan²⁷ A. Khoukaz⁶⁸ R. Kiuchi¹ R. Kliemt¹³ O. B. Kolcu^{62A} B. Kopf³ M. Kuessner³ X. Kui (奎贤)^{1,63}
 N. Kumar²⁶ A. Kupsc^{44,75} W. Kühn³⁷ J. J. Lane⁶⁷ P. Larin¹⁸ A. Lavania²⁶ L. Lavezzi^{74A,74C}
 T. T. Lei (雷天天)^{71,58} Z. H. Lei (雷祚弘)^{71,58} M. Lellmann³⁵ T. Lenz³⁵ C. Li (李聪)⁴³ C. Li (李翠)⁴⁷
 C. H. Li (李春花)³⁹ Cheng Li (李澄)^{71,58} D. M. Li (李德民)⁸⁰ F. Li (李飞)^{1,58} G. Li (李刚)¹ H. B. Li (李海波)^{1,63}
 H. J. Li (李惠静)¹⁹ H. N. Li (李衡讷)^{56j} Hui Li (李慧)⁴³ J. R. Li (李嘉荣)⁶¹ J. S. Li (李静舒)⁵⁹ J. W. Li (李井文)⁵⁰
 K. Li (李科)¹ K. L. Li (李凯璐)¹⁹ L. J. Li (李林健)^{1,63} L. K. Li (李龙科)¹ Lei Li (李蕾)⁴⁸ M. H. Li (李明浩)⁴³
 P. R. Li (李培荣)^{38,k,1} Q. X. Li (李起鑫)⁵⁰ S. X. Li (李素娴)¹² T. Li (李腾)⁵⁰ W. D. Li (李卫东)^{1,63}
 W. G. Li (李卫国)^{1a} X. H. Li (李旭红)^{71,58} X. L. Li (李晓玲)⁵⁰ X. Y. Li (李晓宇)^{1,8} Y. G. Li (李彦谷)^{46,h}
 Z. J. Li (李志军)⁵⁹ Z. X. Li (李振轩)¹⁵ C. Liang (梁畅)⁴² H. Liang (梁浩)^{1,63} H. Liang (梁昊)^{71,58}
 Y. F. Liang (梁勇飞)⁵⁴ Y. T. Liang (梁羽铁)^{31,63} G. R. Liao (廖广睿)¹⁴ L. Z. Liao (廖龙洲)⁵⁰ Y. P. Liao (廖一朴)^{1,63}
 J. Libby²⁶ A. Limphirat⁶⁰ D. X. Lin (林德旭)^{31,63} T. Lin (林韬)¹ B. J. Liu (刘北江)¹ B. X. Liu (刘宝鑫)⁷⁶
 C. Liu (刘成)³⁴ C. X. Liu (刘春秀)¹ F. Liu (刘芳)¹ F. H. Liu (刘福虎)⁵³ Feng Liu (刘峰)⁶ G. M. Liu (刘国明)^{56j}
 H. Liu (刘昊)^{38,k,1} H. B. Liu (刘宏邦)¹⁵ H. H. Liu (刘欢欢)¹ H. M. Liu (刘怀民)^{1,63} Huihui Liu (刘汇慧)²¹
 J. B. Liu (刘建北)^{71,58} J. Y. Liu (刘晶译)^{1,63} K. Liu (刘凯)¹ K. Y. Liu (刘魁勇)⁴⁰ Ke Liu (刘珂)²² L. Liu (刘亮)^{71,58}
 L. C. Liu (刘良辰)⁴³ Lu Liu (刘露)⁴³ M. H. Liu (刘美宏)^{12,g} P. L. Liu (刘佩莲)¹ Q. Liu (刘倩)⁶³
 S. B. Liu (刘树彬)^{71,58} T. Liu (刘桐)^{12,g} W. K. Liu (刘维克)⁴³ W. M. Liu (刘卫民)^{71,58} X. Liu (刘翔)^{38,k,1}
 Y. Liu (刘英)^{38,k,1} Y. Liu (刘义)⁸⁰ Y. B. Liu (刘玉斌)⁴³ Z. A. Liu (刘振安)^{1,58,63} Z. Q. Liu (刘智青)⁵⁰
 X. C. Lou (娄辛丑)^{1,58,63} F. X. Lu (卢飞翔)⁵⁹ H. J. Lu (吕海江)²³ J. G. Lu (吕军光)^{1,58} X. L. Lu (陆小玲)¹
 Y. Lu (卢宇)⁷ Y. P. Lu (卢云鹏)^{1,58} Z. H. Lu (卢泽辉)^{1,63} C. L. Luo (罗成林)⁴¹ M. X. Luo (罗民生)⁷⁹
 T. Luo (罗涛)^{12,g} X. L. Luo (罗小兰)^{1,58} X. R. Lyu (吕晓睿)⁶³ Y. F. Lyu (吕翌丰)⁴³ F. C. Ma (马凤才)⁴⁰
 H. Ma (马衡)⁷⁸ H. L. Ma (马海龙)¹ J. L. Ma (马俊力)^{1,63} L. L. Ma (马连良)⁵⁰ M. M. Ma (马明明)^{1,63}
 Q. M. Ma (马秋梅)¹ R. Q. Ma (马润秋)^{1,63} X. Y. Ma (马晓妍)^{1,58} Y. M. Ma (马玉明)³¹ F. E. Maas¹⁸
 M. Maggiora^{74A,74C} S. Malde⁶⁹ A. Mangoni^{28B} Y. J. Mao (冒亚军)^{46,h} Z. P. Mao (毛泽普)¹ S. Marcello^{74A,74C}
 Z. X. Meng (孟召霞)⁶⁶ J. G. Messchendorp^{13,64} G. Mezzadri^{29A} H. Miao (妙晗)^{1,63} T. J. Min (闵天觉)⁴²
 R. E. Mitchell²⁷ X. H. Mo (莫晓虎)^{1,58,63} B. Moses²⁷ N. Yu. Muchnoi^{4,c} J. Muskalla³⁵ Y. Nefedov³⁶ F. Nerling^{18,e}
 I. B. Nikolaev^{4,c} Z. Ning (宁哲)^{1,58} S. Nisar^{11,m} Q. L. Niu (牛祺乐)^{38,k,1} W. D. Niu (牛文迪)⁵⁵ Y. Niu (牛艳)⁵⁰
 S. L. Olsen⁶³ Q. Ouyang (欧阳群)^{1,58,63} S. Pacetti^{28B,28C} X. Pan (潘祥)⁵⁵ Y. Pan (潘越)⁵⁷ P. Patteri^{28A}
 Y. P. Pei (裴宇鹏)^{71,58} M. Pelizaeus³ H. P. Peng (彭海平)^{71,58} Y. Y. Peng (彭云翊)^{38,k,1} K. Peters^{13,e}
 J. L. Ping (平加伦)⁴¹ R. G. Ping (平荣刚)^{1,63} S. Plura³⁵ V. Prasad³³ F. Z. Qi (齐法制)¹ H. Qi (齐航)^{71,58}
 H. R. Qi (漆红荣)⁶¹ M. Qi (祁鸣)⁴² T. Y. Qi (齐天钰)^{12,g} S. Qian (钱森)^{1,58} W. B. Qian (钱文斌)⁶³
 C. F. Qiao (乔从丰)⁶³ X. K. Qiao (乔晓珂)⁸⁰ J. J. Qin (秦佳佳)⁷² L. Q. Qin (秦丽清)¹⁴ L. Y. Qin (秦龙宇)^{71,58}
 X. P. Qin (覃潇平)^{12,g} X. S. Qin (秦小帅)⁵⁰ Z. H. Qin (秦中华)^{1,58} J. F. Qiu (邱进发)¹ S. Q. Qu (屈三强)⁶¹
 C. F. Redmer³⁵ K. J. Ren (任旷洁)³⁹ A. Rivetti^{74C} M. Rolo^{74C} G. Rong (荣刚)^{1,63} Ch. Rosner¹⁸
 M. Q. Ruan (阮曼奇)^{1,58} S. N. Ruan (阮氏宁)⁴³ N. Salone⁴⁴ A. Sarantsev^{36,d} Y. Schelhaas³⁵ K. Schoenning⁷⁵
 M. Scodreggio^{29A} K. Y. Shan (尚科羽)^{12,g} W. Shan (单葳)²⁴ X. Y. Shan (单心钰)^{71,58} J. F. Shanguan (上官剑锋)⁵⁵
 L. G. Shao (邵立港)^{1,63} M. Shao (邵明)^{71,58} C. P. Shen (沈成平)^{12,g} H. F. Shen (沈宏飞)^{1,8} W. H. Shen (沈文涵)⁶³
 X. Y. Shen (沈肖雁)^{1,63} B. A. Shi (施伯安)⁶³ H. Shi (史华)^{71,58} H. C. Shi (石煌超)^{71,58} J. L. Shi (石家磊)^{12,g}
 J. Y. Shi (石京燕)¹ Q. Q. Shi (石勤强)⁵⁵ X. Shi (史欣)^{1,58} J. J. Song (宋娇娇)¹⁹ T. Z. Song (宋天资)⁵⁹
 W. M. Song (宋维民)^{34,1} Y. J. Song (宋宇镜)^{12,g} Y. X. Song (宋响轩)^{46,h,n} S. Sosio^{74A,74C} S. Spataro^{74A,74C}
 F. Stieler³⁵ Y. J. Su (粟杨捷)⁶³ G. B. Sun (孙光豹)⁷⁶ G. X. Sun (孙功星)¹ H. Sun (孙昊)⁶³ H. K. Sun (孙浩凯)¹
 J. F. Sun (孙俊峰)¹⁹ K. Sun (孙开)⁶¹ L. Sun (孙亮)⁷⁶ S. S. Sun (孙胜森)^{1,63} T. Sun^{51,f} W. Y. Sun (孙文玉)³⁴
 Y. Sun (孙源)⁹ Y. J. Sun (孙勇杰)^{71,58} Y. Z. Sun (孙永昭)¹ Z. T. Sun (孙振田)⁵⁰ C. J. Tang (唐昌建)⁵⁴
 G. Y. Tang (唐光毅)¹ J. Tang (唐健)⁵⁹ Y. A. Tang (唐迎澳)⁷⁶ L. Y. Tao (陶璐燕)⁷² Q. T. Tao (陶秋田)^{25,i} M. Tat⁶⁹

J. X. Teng (滕佳秀)^{71,58} V. Thoren⁷⁵ W. H. Tian (田文辉)⁵² W. H. Tian (田文辉)⁵⁹ Y. Tian (田野)^{31,63}
 Z. F. Tian (田喆飞)⁷⁶ I. Uman^{62B} Y. Wan (万宇)⁵⁵ S. J. Wang (王少杰)⁵⁰ B. Wang (王斌)¹ B. L. Wang (王滨龙)⁶³
 Bo Wang (王博)^{71,58} C. W. Wang (王成伟)⁴² D. Y. Wang (王大勇)^{46,h} F. Wang (王菲)⁷² H. J. Wang (王泓鉴)^{38,k,1}
 J. P. Wang (王吉鹏)⁵⁰ K. Wang (王科)^{1,58} L. L. Wang (王亮亮)¹ L. W. Wang (王璐仪)³⁴ M. Wang (王萌)⁵⁰
 N. Y. Wang (王南洋)⁶³ S. Wang (王顺)^{12,g} S. Wang (王石)^{38,k,1} T. Wang (王婷)^{12,g} T. J. Wang (王腾蛟)⁴³
 W. Wang (王为)⁵⁹ W. Wang (王维)⁷² W. P. Wang (王维平)^{35,58,71,o} X. Wang (王轩)^{46,h} X. F. Wang (王雄飞)^{38,k,1}
 X. J. Wang (王希俊)³⁹ X. L. Wang (王小龙)^{12,g} Y. Wang (王亦)⁶¹ Y. D. Wang (王雅迪)⁴⁵ Y. F. Wang (王贻芳)^{1,58,63}
 Y. L. Wang (王艺龙)¹⁹ Y. N. Wang (王亚男)⁴⁵ Y. Q. Wang (王雨晴)¹ Yaqian Wang (王亚乾)¹⁷ Yi Wang (王义)⁶¹
 Z. Wang (王铮)^{1,58} Z. L. Wang (王治浪)⁷² Z. Y. Wang (王至勇)^{1,63} Ziyi Wang (王子一)⁶³ D. H. Wei (魏代会)¹⁴
 F. Weidner⁶⁸ S. P. Wen (文硕频)¹ C. Wenzel³ U. Wiedner³ G. Wilkinson⁶⁹ M. Wolke⁷⁵ L. Wollenberg³
 C. Wu (吴晨)³⁹ J. F. Wu (吴金飞)^{1,8} L. H. Wu (伍灵慧)¹ L. J. Wu (吴连近)^{1,63} X. Wu (吴潇)^{12,g}
 X. H. Wu (伍雄浩)³⁴ Y. Wu (吴言)^{71,58} Y. H. Wu (吴业昊)⁵⁵ Y. J. Wu (吴英杰)³¹ Z. Wu (吴智)^{1,58}
 L. Xia (夏磊)^{71,58} X. M. Xian (咸秀梅)³⁹ T. Xiang (相腾)^{46,h} D. Xiao (肖栋)^{38,k,1} G. Y. Xiao (肖光延)⁴²
 S. Y. Xiao (肖素玉)¹ Y. L. Xiao (肖云龙)^{12,g} Z. J. Xiao (肖振军)⁴¹ C. Xie (谢陈)⁴² X. H. Xie (谢昕海)^{46,h}
 Y. Xie (谢勇)⁵⁰ Y. G. Xie (谢宇广)^{1,58} Y. H. Xie (谢跃红)⁶ Z. P. Xie (谢智鹏)^{71,58} T. Y. Xing (邢天宇)^{1,63}
 C. F. Xu^{1,63} C. J. Xu (许创杰)⁵⁹ G. F. Xu (许国发)¹ H. Y. Xu (许皓月)^{66,2} M. Xu (徐明)^{71,58} Q. J. Xu (徐庆君)¹⁶
 Q. N. Xu³⁰ W. Xu (许威)¹ W. L. Xu (徐万伦)⁶⁶ X. P. Xu (徐新平)⁵⁵ Y. Xu (徐月)⁴⁰ Y. C. Xu (胥英超)⁷⁷
 Z. P. Xu (许泽鹏)⁴² Z. S. Xu (许昭燊)⁶³ F. Yan (严芳)^{12,g} L. Yan (严亮)^{12,g} W. B. Yan (鄢文标)^{71,58}
 W. C. Yan (闫文成)⁸⁰ X. Q. Yan (严薛强)^{1,63} H. J. Yang (杨海军)^{51,f} H. L. Yang (杨昊霖)³⁴ H. X. Yang (杨洪勋)¹
 T. Yang (杨涛)¹ Y. Yang (杨莹)^{12,g} Y. F. Yang (杨翊凡)^{1,63} Y. F. Yang (杨艳芳)⁴³ Y. X. Yang (杨逸翔)^{1,63}
 Z. W. Yang (杨政武)^{38,k,1} Z. P. Yao (姚志鹏)⁵⁰ M. Ye (叶梅)^{1,58} M. H. Ye (叶铭汉)⁸ J. H. Yin (殷俊昊)¹
 Z. Y. You (尤郑昀)⁵⁹ B. X. Yu (俞伯祥)^{1,58,63} C. X. Yu (喻纯旭)⁴³ G. Yu (余刚)^{1,63} J. S. Yu (俞洁晟)^{25,i}
 T. Yu (于涛)⁷² X. D. Yu (余旭东)^{46,h} Y. C. Yu (于勇超)⁸⁰ C. Z. Yuan (苑长征)^{1,63} L. Yuan (袁丽)²
 S. C. Yuan (苑思成)^{1,63} Y. Yuan (袁野)^{1,63} Z. Y. Yuan (袁朝阳)⁵⁹ C. X. Yue (岳崇兴)³⁹ A. A. Zafar⁷³
 F. R. Zeng (曾凡蕊)⁵⁰ S. H. Zeng (曾胜辉)⁷² X. Zeng (曾鑫)^{12,g} Y. Zeng (曾云)^{25,i} X. Y. Zhai (翟星晔)³⁴
 Y. C. Zhai (翟云聪)⁵⁰ Y. H. Zhan (詹永华)⁵⁹ A. Q. Zhang (张安庆)^{1,63} B. L. Zhang (张伯伦)^{1,63}
 B. X. Zhang (张丙新)¹ D. H. Zhang (张丹昊)⁴³ G. Y. Zhang (张广义)¹⁹ H. Zhang (张豪)^{71,58}
 H. C. Zhang (张航畅)^{1,58,63} H. H. Zhang (张宏宏)³⁴ H. H. Zhang (张宏浩)⁵⁹ H. Q. Zhang (张华桥)^{1,58,63}
 H. Y. Zhang (章红宇)^{1,58} J. Zhang (张晋)⁵⁹ J. Zhang (张进)⁸⁰ J. J. Zhang (张进军)⁵² J. L. Zhang (张杰磊)²⁰
 J. Q. Zhang (张敬庆)⁴¹ J. W. Zhang (张家文)^{1,58,63} J. X. Zhang (张景旭)^{38,k,1} J. Y. Zhang (张建勇)¹
 J. Z. Zhang (张景芝)^{1,63} Jianyu Zhang (张剑宇)⁶³ L. M. Zhang (张黎明)⁶¹ Lei Zhang (张雷)⁴² P. Zhang (张鹏)^{1,63}
 Q. Y. Zhang (张秋岩)^{39,80} S. H. Zhang (张水涵)^{1,63} Shulei Zhang (张书磊)^{25,i} X. D. Zhang (张小东)⁴⁵
 X. M. Zhang (张晓梅)¹ X. Y. Zhang (张学尧)⁵⁰ Y. Zhang (张瑶)¹ Y. Zhang (张宇)⁷² Y. T. Zhang (张亚腾)⁸⁰
 Y. H. Zhang (张银鸿)^{1,58} Y. X. Zhang (张雅璇)⁴³ Yan Zhang (张言)^{71,58} Z. D. Zhang (张正德)¹
 Z. H. Zhang (张泽恒)¹ Z. L. Zhang (张兆领)³⁴ Z. Y. Zhang (张振宇)⁷⁶ Z. Y. Zhang (张子羽)⁴³ G. Zhao (赵光)¹
 J. Y. Zhao (赵静宜)^{1,63} J. Z. Zhao (赵京周)^{1,58} L. Zhao (赵玲)¹ Lei Zhao (赵雷)^{71,58} M. G. Zhao (赵明刚)⁴³
 R. P. Zhao (赵若平)⁶³ S. J. Zhao (赵书俊)⁸⁰ Y. B. Zhao (赵豫斌)^{1,58} Y. X. Zhao (赵宇翔)^{31,63}
 Z. G. Zhao (赵政国)^{71,58} A. Zhemchugov^{36,b} B. Zheng (郑波)⁷² J. P. Zheng (郑建平)^{1,58} W. J. Zheng (郑文静)^{1,63}
 Y. H. Zheng (郑阳恒)⁶³ B. Zhong (钟彬)⁴¹ X. Zhong (钟鑫)⁵⁹ L. P. Zhou (周利鹏)^{1,63} S. Zhou (周帅)⁶
 X. Zhou (周详)⁷⁶ X. K. Zhou (周晓康)⁶ X. R. Zhou (周小蓉)^{71,58} X. Y. Zhou (周兴玉)³⁹
 Y. Z. Zhou (周祎卓)^{12,g} J. Zhu (朱江)⁴³ K. Zhu (朱凯)¹ K. J. Zhu (朱科军)^{1,58,63} L. Zhu (朱林)³⁴
 L. X. Zhu (朱琳萱)⁶³ S. H. Zhu (朱世海)⁷⁰ S. Q. Zhu (朱仕强)⁴² T. J. Zhu (朱腾蛟)^{12,g} Y. C. Zhu (朱莹春)^{71,58}
 Z. A. Zhu (朱自安)^{1,63} J. H. Zou (邹佳恒)¹ J. Zu (祖健)^{71,58}

(BESIII Collaboration)

¹Institute of High Energy Physics, Beijing 100049, China²Beihang University, Beijing 100191, China³Bochum Ruhr-University, D-44780 Bochum, Germany

- ⁴Budker Institute of Nuclear Physics SB RAS (BINP), Novosibirsk 630090, Russia
- ⁵Carnegie Mellon University, Pittsburgh, Pennsylvania 15213, USA
- ⁶Central China Normal University, Wuhan 430079, China
- ⁷Central South University, Changsha 410083, China
- ⁸China Center of Advanced Science and Technology, Beijing 100190, China
- ⁹China University of Geosciences, Wuhan 430074, China
- ¹⁰Chung-Ang University, Seoul, 06974, Republic of Korea
- ¹¹COMSATS University Islamabad, Lahore Campus, Defence Road, Off Raiwind Road, 54000 Lahore, Pakistan
- ¹²Fudan University, Shanghai 200433, China
- ¹³GSI Helmholtzcentre for Heavy Ion Research GmbH, D-64291 Darmstadt, Germany
- ¹⁴Guangxi Normal University, Guilin 541004, China
- ¹⁵Guangxi University, Nanning 530004, China
- ¹⁶Hangzhou Normal University, Hangzhou 310036, China
- ¹⁷Hebei University, Baoding 071002, China
- ¹⁸Helmholtz Institute Mainz, Staudinger Weg 18, D-55099 Mainz, Germany
- ¹⁹Henan Normal University, Xinxiang 453007, China
- ²⁰Henan University, Kaifeng 475004, China
- ²¹Henan University of Science and Technology, Luoyang 471003, China
- ²²Henan University of Technology, Zhengzhou 450001, China
- ²³Huangshan College, Huangshan 245000, China
- ²⁴Hunan Normal University, Changsha 410081, China
- ²⁵Hunan University, Changsha 410082, China
- ²⁶Indian Institute of Technology Madras, Chennai 600036, India
- ²⁷Indiana University, Bloomington, Indiana 47405, USA
- ²⁸INFN Laboratori Nazionali di Frascati, (A)INFN Laboratori Nazionali di Frascati, I-00044, Frascati, Italy; (B)INFN Sezione di Perugia, I-06100, Perugia, Italy; (C)University of Perugia, I-06100, Perugia, Italy
- ²⁹INFN Sezione di Ferrara, (A)INFN Sezione di Ferrara, I-44122, Ferrara, Italy; (B)University of Ferrara, I-44122, Ferrara, Italy
- ³⁰Inner Mongolia University, Hohhot 010021, China
- ³¹Institute of Modern Physics, Lanzhou 730000, China
- ³²Institute of Physics and Technology, Peace Avenue 54B, Ulaanbaatar 13330, Mongolia
- ³³Instituto de Alta Investigación, Universidad de Tarapacá, Casilla 1000000, Chile
- ³⁴Jilin University, Changchun 130012, China
- ³⁵Johannes Gutenberg University of Mainz, Johann-Joachim-Becher-Weg 45, D-55099 Mainz, Germany
- ³⁶Joint Institute for Nuclear Research, 141980 Dubna, Moscow region, Russia
- ³⁷Justus-Liebig-Universität Giessen, II. Physikalisches Institut, Heinrich-Buff-Ring 16, D-35392 Giessen, Germany
- ³⁸Lanzhou University, Lanzhou 730000, China
- ³⁹Liaoning Normal University, Dalian 116029, China
- ⁴⁰Liaoning University, Shenyang 110036, China
- ⁴¹Nanjing Normal University, Nanjing 210023, China
- ⁴²Nanjing University, Nanjing 210093, China
- ⁴³Nankai University, Tianjin 300071, China
- ⁴⁴National Centre for Nuclear Research, Warsaw 02-093, Poland
- ⁴⁵North China Electric Power University, Beijing 102206, China
- ⁴⁶Peking University, Beijing 100871, China
- ⁴⁷Qufu Normal University, Qufu 273165, China
- ⁴⁸Renmin University of China, Beijing 100872, China
- ⁴⁹Shandong Normal University, Jinan 250014, China
- ⁵⁰Shandong University, Jinan 250100, China
- ⁵¹Shanghai Jiao Tong University, Shanghai 200240, China
- ⁵²Shanxi Normal University, Linfen 041004, China
- ⁵³Shanxi University, Taiyuan 030006, China
- ⁵⁴Sichuan University, Chengdu 610064, China
- ⁵⁵Soochow University, Suzhou 215006, China
- ⁵⁶South China Normal University, Guangzhou 510006, China
- ⁵⁷Southeast University, Nanjing 211100, China
- ⁵⁸State Key Laboratory of Particle Detection and Electronics, Beijing 100049, Hefei 230026, PChina
- ⁵⁹Sun Yat-Sen University, Guangzhou 510275, China
- ⁶⁰Suranaree University of Technology, University Avenue 111, Nakhon Ratchasima 30000, Thailand
- ⁶¹Tsinghua University, Beijing 100084, China
- ⁶²Turkish Accelerator Center Particle Factory Group, (A)Istinye University, 34010, Istanbul, Turkey; (B)Near East University, Nicosia, North Cyprus, 99138, Mersin 10, Turkey
- ⁶³University of Chinese Academy of Sciences, Beijing 100049, China
- ⁶⁴University of Groningen, NL-9747 AA Groningen, The Netherlands
- ⁶⁵University of Hawaii, Honolulu, Hawaii 96822, USA
- ⁶⁶University of Jinan, Jinan 250022, China
- ⁶⁷University of Manchester, Oxford Road, Manchester, M13 9PL, United Kingdom
- ⁶⁸University of Muenster, Wilhelm-Klemm-Strasse 9, 48149 Muenster, Germany
- ⁶⁹University of Oxford, Keble Road, Oxford OX13RH, United Kingdom

⁷⁰University of Science and Technology Liaoning, Anshan 114051, China⁷¹University of Science and Technology of China, Hefei 230026, China⁷²University of South China, Hengyang 421001, China⁷³University of the Punjab, Lahore-54590, Pakistan⁷⁴University of Turin and INFN, (A)University of Turin, I-10125, Turin, Italy; (B)University of Eastern Piedmont, I-15121, Alessandria, Italy; (C)INFN, I-10125, Turin, Italy⁷⁵Uppsala University, Box 516, SE-75120 Uppsala, Sweden⁷⁶Wuhan University, Wuhan 430072, China⁷⁷Yantai University, Yantai 264005, China⁷⁸Yunnan University, Kunming 650500, China⁷⁹Zhejiang University, Hangzhou 310027, China⁸⁰Zhengzhou University, Zhengzhou 450001, China^aDeceased^bAlso at the Moscow Institute of Physics and Technology, Moscow 141700, Russia^cAlso at the Novosibirsk State University, Novosibirsk, 630090, Russia^dAlso at the NRC "Kurchatov Institute", PNPI, 188300, Gatchina, Russia^eAlso at Goethe University Frankfurt, 60323 Frankfurt am Main, Germany^fAlso at Key Laboratory for Particle Physics, Astrophysics and Cosmology, Ministry of Education; Shanghai Key Laboratory for Particle Physics and Cosmology; Institute of Nuclear and Particle Physics, Shanghai 200240, China^gAlso at Key Laboratory of Nuclear Physics and Ion-beam Application (MOE) and Institute of Modern Physics, Fudan University, Shanghai 200443, China^hAlso at State Key Laboratory of Nuclear Physics and Technology, Peking University, Beijing 100871, ChinaⁱAlso at School of Physics and Electronics, Hunan University, Changsha 410082, China^jAlso at Guangdong Provincial Key Laboratory of Nuclear Science, Institute of Quantum Matter, South China Normal University, Guangzhou 510006, China^kAlso at MOE Frontiers Science Center for Rare Isotopes, Lanzhou University, Lanzhou 730000, China^lAlso at Lanzhou Center for Theoretical Physics, Lanzhou University, Lanzhou 730000, China^mAlso at the Department of Mathematical Sciences, IBA, Karachi 75270, PakistanⁿAlso at Ecole Polytechnique Federale de Lausanne (EPFL), CH-1015 Lausanne, Switzerland^oAlso at Helmholtz Institute Mainz, Staudinger Weg 18, D-55099 Mainz, Germany

Abstract: Using an electron-positron collision data sample corresponding to $(1.0087 \pm 0.0044) \times 10^{10}$ J/ψ events collected using the BESIII detector at the BEPCII collider, we firstly search for the lepton number violation decay $\phi \rightarrow \pi^+\pi^+e^-e^-$ via $J/\psi \rightarrow \phi\eta$. No obviously signals are found. The upper limit on the branching fraction of $\phi \rightarrow \pi^+\pi^+e^-e^-$ is set to be 1.3×10^{-5} at the 90% confidence level.

Keywords: Lepton number violation, matter anti-matter asymmetry, neutrinoless double beta decay

DOI: 10.1088/1674-1137/ada350 **CSTR:** 32044.14.ChinesePhysicsC.49043001

I. INTRODUCTION

Matter-antimatter asymmetry [1] is a primary issue in the standard cosmology model. According to the Big Bang theory [2], matter and antimatter in the universe should be produced equally and exist in equal amounts. However, observations show that the number of baryons in the universe is $10^9 - 10^{10}$ [3] times that of antibaryons. Sakharov proposed the three conditions to understand this puzzle [4], the first of which is that the baryon number conservation must be violated. Consequently, several baryon number violation (BNV) searches have been conducted at collider experiments and specially designed non-collider experiments, such as proton decay experiments; however, no positive results have been obtained. Many theories [5, 6] pointed out that if BNV occurs, the lepton number should also be violated (LNV). This provides another perspective on exploring the asymmetry between matter and antimatter in the universe.

Conversely, neutrino oscillation experiments [7–10] show that neutrinos have tiny masses, which proves that

the Standard Model (SM) cannot fully describe the neutrino sector. Some of the SM extensions believe that neutrinos may have majorana components whose particle and antiparticle are identical [11]. This may lead to LNV processes with $\Delta L = 2$, such as neutrinoless double beta decay ($0\nu 2\beta$) [12]. Although hadrons comprising first generation quarks have been well explored in $0\nu 2\beta$, constraints on the LNV process [13–18] suggest that searching for LNV with non-first generation quark decays at collider experiments would be necessary.

Many recent collider experiments, such as NA62 [19], E865 [20], LHCb [21], CMS [22], ATLAS [23], CLEO [24] and BESIII [25], have searched for LNV processes. Among them, references [19, 20] reported LNV with second generation quark decays in K mesons. However, no significant evidence of a possible LNV effect has been observed yet. Complementary to those measurements, the study of LNV using ϕ decays is distinctive owing to the different phase space (PHSP) it explores. In this study, we analyze the $(1.0087 \pm 0.0044) \times 10^{10}$ J/ψ data sample collected with the BESIII detector [26] operating at the

BEPCII storage ring [27] to search for the SM forbidden LNV decay of $\phi \rightarrow \pi^+\pi^+e^-e^-$. The charge conjugate channel is always implied throughout this study.

II. BESIII DETECTOR AND MONTE CARLO SIMULATION

The BESIII detector [26] records symmetric e^+e^- collisions provided by the BEPCII storage ring [27] in the center-of-mass energy range from 1.85 to 4.95 GeV, with a peak luminosity of $1.1 \times 10^{33} \text{ cm}^{-2}\text{s}^{-1}$ achieved at $\sqrt{s} = 3.773 \text{ GeV}$. BESIII has collected large data samples in this energy region [28]. The cylindrical core of the BESIII detector covers 93% of the full solid angle and comprises a helium-based multilayer drift chamber (MDC), a plastic scintillator time-of-flight system (TOF), and a CsI(Tl) electromagnetic calorimeter (EMC), all enclosed in a superconducting solenoidal magnet providing a 1.0 T magnetic field. The magnetic field was 0.9 T in 2012, which affects 11% of the total J/ψ data. The solenoid is supported by an octagonal flux-return yoke with resistive plate counter muon identification modules interleaved with steel. The charged-particle momentum resolution at 1 GeV/c is 0.5%, and the specific ionization energy loss (dE/dx) resolution is 6% for electrons from Bhabha scattering. The EMC measures photon energies with a resolution of 2.5% (5%) at 1 GeV in the barrel (end cap) region. The time resolution in the TOF barrel region is 68 ps, while that in the end cap region is 110 ps. The end cap TOF system was upgraded in 2015 using multigap resistive plate chamber technology, providing a time resolution of 60 ps, which benefits 87% of the data used in this analysis [29].

Simulated Monte Carlo (MC) samples produced with GEANT4-based [30] software, which includes the geometric description of the BESIII detector [31] and the detector response, are used to determine the detection efficiency and to estimate the background contributions. The simulation includes the beam-energy spread and initial-state radiation (ISR) in the e^+e^- annihilation modeled with the generator KKMC [32, 33]. The inclusive MC simulation sample includes the production of the J/ψ resonance and the continuum processes incorporated in KKMC [32, 33]. The known decay modes are modeled with EVTGEN [34, 35] using world averaged branching fraction values [36], and the remaining unknown decays from the charmonium states with LUNDCHARM [37, 38]. Final-state radiation from charged final-state particles is incorporated with PHOTOS [39].

III. DATA ANALYSIS

A. Method

In this analysis, we search for the decay $\phi \rightarrow \pi^+\pi^+e^-e^-$

via $J/\psi \rightarrow \phi\eta, \eta \rightarrow \gamma\gamma$. In order to avoid the large uncertainty from $\mathcal{B}(J/\psi \rightarrow \phi\eta)$ [36], which is approximately 11%, we measure the branching fraction of the signal decay $\phi \rightarrow \pi^+\pi^+e^-e^-$ relative to that of the reference channel $\phi \rightarrow K^+K^-$ via $J/\psi \rightarrow \phi\eta$.

The branching fractions of $\phi \rightarrow \pi^+\pi^+e^-e^-$ and $\phi \rightarrow K^+K^-$ can be written as

$$\mathcal{B}(\phi \rightarrow \pi^+\pi^+e^-e^-) = \frac{N_{\pi^+\pi^+e^-e^-}^{\text{net}}/\varepsilon_{\pi^+\pi^+e^-e^-}}{N^{\text{tot}} \times \mathcal{B}(J/\psi \rightarrow \phi\eta) \times \mathcal{B}(\eta \rightarrow \gamma\gamma)}, \quad (1)$$

and

$$\mathcal{B}(\phi \rightarrow K^+K^-) = \frac{N_{K^+K^-}^{\text{net}}/\varepsilon_{K^+K^-}}{N^{\text{tot}} \times \mathcal{B}(J/\psi \rightarrow \phi\eta) \times \mathcal{B}(\eta \rightarrow \gamma\gamma)}, \quad (2)$$

respectively, where $N_{\pi^+\pi^+e^-e^-}^{\text{net}}$ and $N_{K^+K^-}^{\text{net}}$ are the signal yields, N^{tot} is the total number of J/ψ events, and $\varepsilon_{\pi^+\pi^+e^-e^-}$ and $\varepsilon_{K^+K^-}$ are the detection efficiencies for the $J/\psi \rightarrow \eta\phi, \eta \rightarrow \gamma\gamma, \phi \rightarrow \pi^+\pi^+e^-e^-$ and $J/\psi \rightarrow \eta\phi, \eta \rightarrow \gamma\gamma, \phi \rightarrow K^+K^-$, respectively. $\mathcal{B}(J/\psi \rightarrow \phi\eta)$ and $\mathcal{B}(\eta \rightarrow \gamma\gamma)$ are the branching fractions of $J/\psi \rightarrow \phi\eta$ and $\eta \rightarrow \gamma\gamma$. Using the two equations above, the branching fraction of $\phi \rightarrow \pi^+\pi^+e^-e^-$ can be determined by

$$\mathcal{B}(\phi \rightarrow \pi^+\pi^+e^-e^-) = \mathcal{B}(\phi \rightarrow K^+K^-) \times \frac{N_{\pi^+\pi^+e^-e^-}^{\text{net}}/\varepsilon_{\pi^+\pi^+e^-e^-}}{N_{K^+K^-}^{\text{net}}/\varepsilon_{K^+K^-}}, \quad (3)$$

where $\mathcal{B}(\phi \rightarrow K^+K^-) = (49.2 \pm 0.5)\%$ [36]. The total systematic uncertainty can be reduced significantly because the uncertainty of the input $\mathcal{B}(\phi \rightarrow K^+K^-)$ is only 1.0%.

B. Analysis of $\phi \rightarrow K^+K^-$

The reference decay $J/\psi \rightarrow \phi\eta$ is reconstructed with $\eta \rightarrow \gamma\gamma$ and $\phi \rightarrow K^+K^-$. In each event, at least two charged tracks and two neutral candidates are required.

Charged tracks detected in the MDC are required to be within a polar angle (θ) range of $|\cos\theta| < 0.93$, where θ is defined with respect to the z -axis, which is the symmetry axis of the MDC. The distance of closest approach to the interaction point (IP) must be less than 10 cm along the z -axis, $|V_z|$, and less than 1 cm in the transverse plane, $|V_{xy}|$. Events with exactly two good charged tracks with zero net charge are kept for further analysis. For charged particle identification (PID), we use a combination of the dE/dx in the MDC, and the time of flight in the TOF to calculate the Confidence Level (CL) for pion and kaon hypotheses (CL_π and CL_K). For kaon candidates, they are required to satisfy $CL_K > 0.001$ and $CL_K > CL_\pi$ to avoid contamination from pions and to suppress background.

The photon candidates are selected from isolated EMC clusters. The clusters are required to start within 700 ns after the event start time and fall outside a cone

angle of 20° around the nearest extrapolated good charged track to suppress electronic noise and beam related background. The minimum energy of each EMC cluster is required to be greater than 25 MeV in the barrel region ($|\cos\theta| < 0.80$) or 50 MeV in the end-cap regions ($0.86 < |\cos\theta| < 0.92$). The η candidate is reconstructed by $\eta \rightarrow \gamma\gamma$, where the invariant mass of the $\gamma\gamma$ pair is required to satisfy $0.45 \text{ GeV}/c^2 < M_{\gamma\gamma} < 0.65 \text{ GeV}/c^2$. A kinematic fit is performed to reduce backgrounds and improve mass resolution by constraining the total four momentum (4C) to that of the initial e^+e^- beams under the hypothesis of $e^+e^- \rightarrow K^+K^-\gamma\gamma$. All good photons are looped over together with the two tracks in the kinematic fit, and the candidate with the least χ^2 is retained for further analysis.

To obtain the signal yield of $\phi \rightarrow K^+K^-$, we fit the $M_{K^+K^-}$ distribution of the accepted candidate events in the η signal region ($[0.525, 0.565] \text{ GeV}/c^2$) and in the η sideband region ($[0.452, 0.492] \text{ GeV}/c^2$ or $[0.598, 0.638] \text{ GeV}/c^2$). The signal region is determined by $[\mu - 3\sigma, \mu + 3\sigma]$; the sideband region is outside the signal region and the distance between the two intervals is 5σ , where μ and σ are the mean and standard deviation obtained from a Gaussian fit to the $M_{\gamma\gamma}$ distribution, as shown in Fig. 1. In the fits to the $M_{K^+K^-}$ distribution in the η signal region, the signal shape is described by a MC shape convolved with a double Gaussian function and the background shape is described by second-order polynomial function. In the fits to the $M_{K^+K^-}$ distribution in the η sideband region, the signal shape is described by a MC shape convolved with a double Gaussian function, and the background shape is described by an inverted ARGUS function [40] multiplied by a fourth-order polynomial function. The double Gaussian function and the background model parameters float in the fits. With the numbers of N_{signal} and N_{sideband} obtained from the fits in Fig. 2, the net

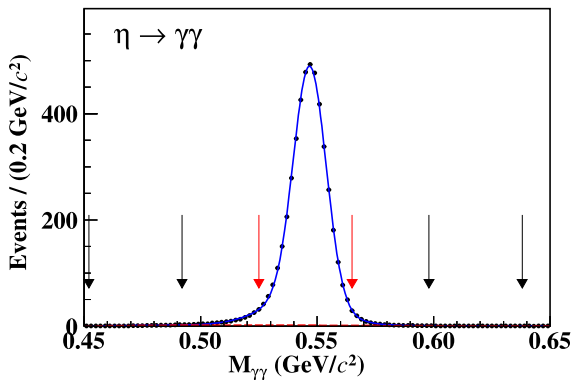


Fig. 1. (color online) Fit to the $M_{\gamma\gamma}$ distribution, where the black points represent the signal MC candidates, the blue curve is the fit result, the red dashed line is the second-order polynomial background, the red arrows show the signal region, and the black arrows show the sideband region.

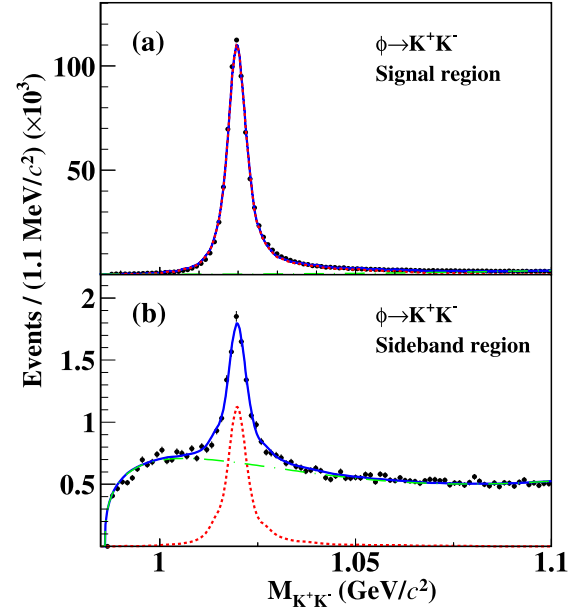


Fig. 2. (color online) Invariant mass $M_{K^+K^-}$ distributions of $J/\psi \rightarrow \phi\eta$ candidates in the (a) signal and (b) sideband region of η , with fit results overlaid. The black points represent the data, the blue curves are the fit results, the green dash-dotted curves are the fitted background shapes, and the red dotted curves are the signal shapes.

number of the $\phi \rightarrow K^+K^-$ candidate events is calculated by

$$N_{K^+K^-}^{\text{net}} = N_{\text{signal}} - \frac{1}{2} \times N_{\text{sideband}} = 823764 \pm 1023. \quad (4)$$

Here, $\frac{1}{2} \times N_{\text{sideband}}$ is the background yield under the $M_{\gamma\gamma}$ signal region, where the scale factor of 1/2 is determined under the assumption that the background is flat in the $M_{\gamma\gamma}$ distribution.

To determine the detection efficiency, the $J/\psi \rightarrow \phi\eta$ ($\phi \rightarrow K^+K^-$, $\eta \rightarrow \gamma\gamma$) decays are simulated, where the decays of $J/\psi \rightarrow \phi\eta$, $\phi \rightarrow K^+K^-$, and $\eta \rightarrow \gamma\gamma$ are modeled by a helicity amplitude generator HELAMP, a VSS model (decay of a vector particle to a pair of scalars), and a PHSP generator, respectively [41]. After applying all the selection criteria, we fit the invariant mass of the K^+K^- combination ($M_{K^+K^-}$) for the survived signal MC events in the signal and sideband regions, respectively. In the fits, the signal shape is modeled by a MC shape convolved with a double Gaussian function and the background is described by a second-order polynomial function. The number of observed signal events is obtained to be $N_{\text{obs}}^{\text{MC}} = N_{\phi \rightarrow K^+K^-}^{\text{signal}} - \frac{1}{2} \times N_{\phi \rightarrow K^+K^-}^{\text{sideband}}$, where $N_{\phi \rightarrow K^+K^-}^{\text{signal}}$ and $N_{\phi \rightarrow K^+K^-}^{\text{sideband}}$ are the observed numbers in the η signal and sideband regions, respectively. Dividing it by the number of total signal MC events $N_{\text{total}}^{\text{MC}}$, the efficiency of detecting the decays of $\phi \rightarrow K^+K^-$ is

$$\varepsilon_{KK} = \frac{N_{\text{obs}}^{\text{MC}}}{N_{\text{total}}^{\text{MC}}} = \frac{471297}{1000000} = (47.1 \pm 0.1)\%. \quad (5)$$

C. Analysis of $\phi \rightarrow \pi^+\pi^+e^-e^-$

The LNV decay of $\phi \rightarrow \pi^+\pi^+e^-e^-$ is searched through $J/\psi \rightarrow \phi\eta$, where the η candidate is reconstructed through $\eta \rightarrow \gamma\gamma$. In each event, at least four charged tracks and two neutral candidates are required.

The good charged tracks are selected using the same criteria as those used in the reference mode. For charged PID, we use a combination of the dE/dx in the MDC, the time of flight in the TOF, and the energy and shape of clusters in the EMC to calculate the CL for the electron, pion, and kaon hypotheses (CL_e , CL_π , and CL_K). The electron candidates are required to satisfy $CL_e > 0.001$ and $CL_e/(CL_e + CL_K + CL_\pi) > 0.8$. Furthermore, to suppress background from pions, electrons must satisfy an additional requirement $E/p > 0.8$ for tracks with $p_e \geq 0.5$ GeV/c, where E and p represent the energy deposited in the EMC and the momentum reconstructed in the MDC, respectively. Pion candidates are required to satisfy $CL_\pi > 0$ and $CL_\pi > CL_K$. The good photons are selected in the same way as in the reference mode.

A kinematic fit is performed to reduce backgrounds and improve the mass resolution by constraining the total four momentum (4C) to that of the initial e^+e^- beams. All the good photons are looped over together with the four tracks in the kinematic fit. To suppress the combinatorial background, the χ^2 of the 4C kinematic fit is required to be less than 30, determined via the Punzi significance method [42] using the formula $\frac{\varepsilon}{1.5 + \sqrt{B}}$, where ε is the detection efficiency and B is the number of background events from the inclusive MC sample. If more than one combination is obtained, the combination with the minimum χ^2 is retained.

We perform 4C kinematic fits under six different hypotheses of $J/\psi \rightarrow \pi^+\pi^+e^-e^- \gamma\gamma$, $K^+K^-K^+K^- \gamma\gamma$, $K^+K^-p\bar{p}\gamma\gamma$, $K^+K^-\pi^+\pi^-\gamma\gamma$, $\pi^+\pi^-\pi^+\pi^-\gamma\gamma$, and $\pi^+\pi^-\rho\bar{\rho}\gamma\gamma$ to suppress the contamination of the final states with four charged tracks from mis-identification. If the kinematic fit for the $\pi^+\pi^+e^-e^- \gamma\gamma$ hypotheses is successful and gives the minimum χ^2 among these six assignments, the event is then accepted for further analysis.

To further suppress possible background from γ -conversion, the opening angle $\theta_{\pi e}$ between any pions (possibly mis-identified from real positrons) and electrons are required to be greater than 8° .

Based on a fit with a double Gaussian function and a Chebychev polynomial to model the signal and background shapes of the simulated $M_{\pi^+\pi^+e^-e^-}$ and $M_{\gamma\gamma}$ distributions, the signal region is determined to be $[0.99, 1.04]$ GeV/ c^2 for $M_{\pi^+\pi^+e^-e^-}$ and $[0.52, 0.57]$ GeV/ c^2 for $M_{\gamma\gamma}$. This corresponds to a range of ± 3 times the mass resolu-

tion around their known masses [36]. The detection efficiency is determined to be 4.40% with simulated $J/\psi \rightarrow \phi\eta \rightarrow (\pi^+\pi^+e^-e^-)(\gamma\gamma)$ events, where the J/ψ decay is modeled by a helicity amplitude generator HELAMP [41] and the ϕ/η decays are modeled by a phase space (PHSP) generator.

Using TopoAna, an event type analysis tool [43], the backgrounds from J/ψ decays are investigated using an inclusive MC simulation sample, which has the same size as the J/ψ data sample. Only 39 events from 14 different decay channels remain. The distribution of $M_{\pi^+\pi^+e^-e^-}$ for the background events from the inclusive MC simulation sample is shown in Fig. 3, where the red arrows show the signal region. No background event is observed in the signal region.

To avoid the influence of statistical fluctuation, large exclusive MC simulation samples for the three main background channels, (1) $J/\psi \rightarrow \pi^+\pi^-\eta\gamma^F$, $\eta \rightarrow e^+e^-\gamma^F$ (γ^F is the γ from final state radiation), (2) $J/\psi \rightarrow \eta'$, $\eta' \rightarrow \pi^+\pi^-\eta$, $\eta \rightarrow e^+e^-$, and (3) $J/\psi \rightarrow \pi^+\eta b_1^-$, $\eta \rightarrow \gamma\gamma$, $b_1^- \rightarrow \pi^-\omega$, $\omega \rightarrow e^+e^-$, are produced. Furthermore, the possibility of background from other ϕ decays, such as $J/\psi \rightarrow \phi\eta$, $\phi \rightarrow e^+e^-\eta$, $\eta \rightarrow \gamma\gamma$, is also investigated. No background event is found near the signal region under the current MC sample statistics. Figure 4 shows the two dimensional distribution of $M_{\gamma\gamma}$ versus $M_{\pi^+\pi^+e^-e^-}$ of the accepted $\phi \rightarrow \pi^+\pi^+e^-e^-$ candidate events in the data. No event is observed in the signal region.

IV. SYSTEMATIC UNCERTAINTY

The sources of systematic uncertainties for the product branching fractions include MDC tracking, charged PID, 4C kinematic fit, χ^2 requirement, $\theta_{\pi e}$ requirement, signal window, fitting procedure, MC modeling, $N_{K^+K^-}^{\text{net}}$ determination, and $\mathcal{B}(\phi \rightarrow K^+K^-)$. All the sys-

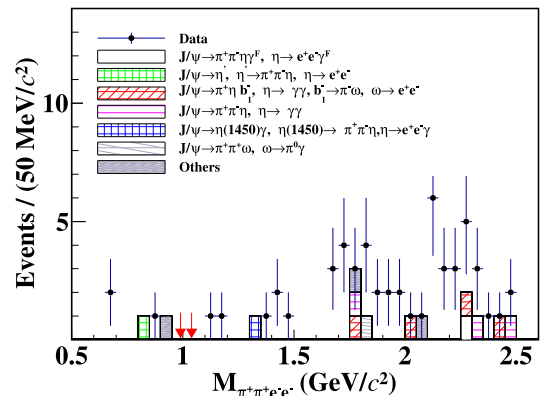


Fig. 3. (color online) The distribution of $M_{\pi^+\pi^+e^-e^-}$ for events in the range of $M_{\gamma\gamma} \in (0.52, 0.57)$ GeV/ c^2 , where the points with error bars are data, the histogram in different styles represent different sources of background modes shown in the legends. The red arrows show the signal region.

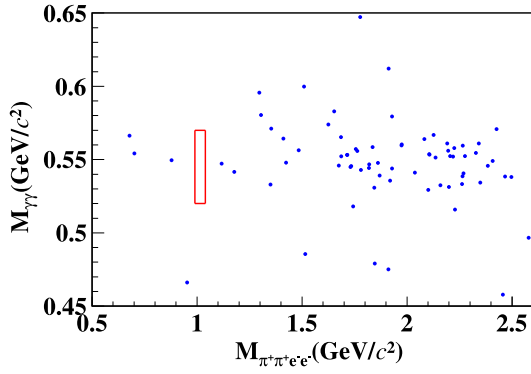


Fig. 4. (color online) The distribution of $M_{\gamma\gamma}$ versus $M_{\pi^+\pi^-e^+e^-}$ of the accepted $\phi \rightarrow \pi^+\pi^-e^+e^-$ candidate events in data. The red box indicates the signal region defined as $[0.99, 1.04]$ GeV/ c^2 for $M_{\pi^+\pi^-e^+e^-}$ and $[0.52, 0.57]$ GeV/ c^2 for $M_{\gamma\gamma}$.

tematic uncertainties are summarized in Table 1, and the total uncertainty is obtained by adding the individual components in quadrature.

The systematic uncertainties of photon detection and quoted branching fractions ($\mathcal{B}(J/\psi \rightarrow \phi\eta)$ and $\mathcal{B}(\eta \rightarrow \gamma\gamma)$) are canceled based Eq. (3).

The uncertainties in tracking efficiency are estimated using the control samples $J/\psi \rightarrow \pi^+\pi^-\pi^0$, $J/\psi \rightarrow e^+e^-$ (γ_{FSR} (γ_{FSR} is the FSR photon), and $J/\psi \rightarrow \pi^0 K^+ K^-$, and are determined to be 0.3% per pion, 0.7% per electron, and 0.3% per kaon, considering the efficiency differences between the data and MC simulations, respectively. Similarly, the uncertainties of PID are 1.0%, 1.0%, and 1.1% for each charged electron, pion, and kaon, respectively. After adding the systematic uncertainties of each track linearly, the total systematic uncertainties in tracking efficiency and PID efficiency are obtained to be 2.6% and 6.2%, respectively.

The systematic uncertainty due to the 4C kinematic fit for $J/\psi \rightarrow \phi\eta \rightarrow K^+ K^- \eta$ ($\eta \rightarrow \gamma\gamma$) is studied by using the control sample of the $J/\psi \rightarrow K^+ K^- \pi^0$ ($\pi^0 \rightarrow \gamma\gamma$) decay mode. The corresponding uncertainty is estimated to be 0.2% by comparing the efficiency differences between the data and MC simulation. Similarly, the systematic uncertainty due to the 4C kinematic fit and $\chi^2 < 30$ for $J/\psi \rightarrow \phi\eta \rightarrow \pi^+\pi^-e^+e^-\eta$ ($\eta \rightarrow \gamma\gamma$) is studied using the control sample of the $J/\psi \rightarrow \pi^+\pi^-\pi^+\pi^-\eta$ ($\eta \rightarrow \gamma\gamma$) decay mode. The corresponding uncertainty is assigned to be 2.3%.

The uncertainty of the $\theta_{\pi e}$ requirement is estimated by varying the optimized requirement $\theta_{\pi e} > 8^\circ$ with alternative $\theta_{\pi e}$ requirements, i.e., $\theta_{\pi e} > 3^\circ$, $\theta_{\pi e} > 4^\circ$, ..., $\theta_{\pi e} > 12^\circ$, $\theta_{\pi e} > 13^\circ$. The largest standard deviation on the detection efficiency, 4.1%, is taken as the corresponding systematic uncertainty.

We use different signal window ranges, such as $\pm 3.1\sigma$, $\pm 3.2\sigma$, and $\pm 2.8\sigma$, to investigate the systematic

Table 1. Relative systematic uncertainties in the branching fraction measurement.

Source	Uncertainty (%)
MDC tracking	2.6
PID	6.2
4C kinematic fit for $\phi \rightarrow K^+ K^-$	0.2
4C kinematic fit for $\phi \rightarrow \pi^+\pi^-e^+e^-$	2.3
$\theta_{\pi e}$ selection requirement	4.1
Signal window	0.2
Yield of $\phi \rightarrow K^+ K^-$	1.1
MC modeling	1.9
$\mathcal{B}(\phi \rightarrow K^+ K^-)$	1.0
Total	8.6

uncertainty due to the selected η signal window. The standard deviation on a detection efficiency of 0.2% is taken as the uncertainty.

The systematic uncertainty of the yield of the reference decay $J/\psi \rightarrow \phi\eta, \phi \rightarrow K^+ K^-$ includes the fit range, signal shape, and background shape. The uncertainty due to the fit range of M_{KK} is estimated by changing the fit from (0.99, 1.10) GeV/ c^2 to (0.99, 1.09) GeV/ c^2 and (0.98, 1.10) GeV/ c^2 . The uncertainty due to the background shape is estimated by changing the second-order polynomial function to a first-order polynomial function. We use alternative signal shapes (an MC shape convolved with a Gaussian function) to estimate the systematic uncertainty due to signal shape. The relative difference between the signal yield and the detection efficiency is taken as the corresponding systematic uncertainty. Consequently, the systematic uncertainties are determined to be 1.0%, 0.1%, and 0.3% for fit range, background shape, and signal shape, respectively. After adding them in quadrature, the total systematic uncertainty associated with the fit procedure is obtained as 1.1%.

An intermediate majorana neutrino ν_N is assumed to decay into π^+e^- to estimate the uncertainty related to the MC simulation model. However, the mass of ν_N remains unknown and can range from the πe mass threshold to the largest available phase space of ϕ decay, which needs to satisfy $m_e + m_\pi \leq m_{\nu_N} \leq \frac{m_\phi}{2}$. We divide the mass range (0.150, 0.50) GeV into 14 equidistant intervals, with a step of 0.025 GeV, i.e., 0.175 GeV, 0.200 GeV, ..., 0.500 GeV. The detection efficiency is averaged to be $(4.32 \pm 0.09)\%$. The difference between this value and the detection efficiency obtained by the PHSP model of 1.9% is taken as the associated systematic uncertainty.

The uncertainty of the quoted branching fraction $\mathcal{B}(\phi \rightarrow K^+ K^-)$ is 1.0% [36].

V. RESULT

Because no event is observed in the signal region, the signal yield (N^{sig}) and background yield (N^{bkg}) are determined to be 0. The upper limit on the signal yield $N_{\pi^+\pi^+e^-e^-}^{\text{up}}$ is estimated to be 45.4 at the 90% CL by utilizing a frequentist method [44] with unbounded profile likelihood treatment of systematic uncertainties, where the background fluctuation is assumed to follow a Poisson distribution, the detection efficiency ($\varepsilon_{\pi^+\pi^+e^-e^-} = 4.40\%$) is assumed to follow a Gaussian distribution, and the systematic uncertainty ($\Delta_{\text{sys}} = 8.6\%$) is considered as the standard deviation of the efficiency.

The upper limit on the branching fraction of $\phi \rightarrow \pi^+\pi^+e^-e^-$ is determined by

$$\mathcal{B}(\phi \rightarrow \pi^+\pi^+e^-e^-) < \mathcal{B}(\phi \rightarrow K^+K^-) \times \frac{N_{\pi^+\pi^+e^-e^-}^{\text{up}}}{N_{K^+K^-}^{\text{net}}/\varepsilon_{K^+K^-}},$$

where $\varepsilon_{K^+K^-} = 47.1\%$, $N_{K^+K^-}^{\text{net}} = 823764 \pm 1023$, $\mathcal{B}(\phi \rightarrow$

$K^+K^-) = (49.2 \pm 0.5)\%$ [34] and $N_{\pi^+\pi^+e^-e^-}^{\text{up}} = 45.4$. Thus, the upper limit on the branching fraction is set to be

$$\mathcal{B}(\phi \rightarrow \pi^+\pi^+e^-e^-) < 1.3 \times 10^{-5}.$$

VI. SUMMARY

In summary, by analyzing $(1.0087 \pm 0.0044) \times 10^{10}$ J/ψ events collected using the BESIII detector at the BEPCII collider, we conduct a novel search for the LNV decay $\phi \rightarrow \pi^+\pi^+e^-e^-$ via $J/\psi \rightarrow \phi\eta$. No obvious signal event is observed and the upper limit on the branching fraction of this decay is set to be 1.3×10^{-5} at the 90% CL. This is the first LNV signal constraint in ϕ meson decays. Our study findings improve the experimental knowledge of LNV decay for hadrons composed of second generation quarks.

References

- [1] F. W. Stecker, arXiv: [hep-ph/0207323](#)
- [2] J. Allday, *Quarks, Leptons and the Big Bang*, (IOP Publishing Ltd., 2002), ISBN: 0-7503-0806-0
- [3] F. C. Adams and G. Laughlin, *Rev. Mod. Phys.* **69**, 337 (1997)
- [4] A. D. Sakharov, *JETP Lett.* **5**, 24 (1967)
- [5] S. Weinberg, *Phys. Rev. Lett.* **43**, 1566 (1979)
- [6] Frank Wilczek and A. Zee, *Phys. Lett. B* **88**, 311 (1979)
- [7] Y. Fukuda *et al.* (Super-Kamiokande Collaboration), *Phys. Rev. Lett.* **81**, 1562 (1998)
- [8] Q. R. Ahmad *et al.* (SNO Collaboration), *Phys. Rev. Lett.* **89**, 011301 (2002)
- [9] K. Eguchi *et al.* (KamLAND Collaboration), *Phys. Rev. Lett.* **90**, 021802 (2003)
- [10] F. P. An *et al.* (KamLAND Collaboration), *Phys. Rev. Lett.* **108**, 171803 (2012)
- [11] E. Majorana, *Nuovo Cimento* **14**, 171 (1937)
- [12] W. H. Furry, *Phys. Rev.* **56**, 1184 (1939)
- [13] F. T. Avignone, S. R. Elliott, and J. Engel, *Rev. Mod. Phys.* **80**, 481 (2008)
- [14] B. T. Zhang *et al.* (CDEX Collaboration), arXiv: [2305.00894](#)
- [15] B. Cropper, *Transfer Reaction Spectroscopy on Neutrinoless Double-Beta Decay Candidate Nuclei*
- [16] I. J. Arnquist *et al.* (MAJORANA Collaboration), arXiv: [2306.01965](#)
- [17] Z. H. Zhao, L. Zhang, and Y. Gao, *Commun. Theor. Phys.* **75**(6), 065202 (2023)
- [18] P. Novella *et al.* (NEXT Collaboration), arXiv: [2305.09435](#)
- [19] R. Aliberti *et al.* (NA62 Collaboration), *Phys. Rev. Lett.* **127**, 131802 (2021)
- [20] R. Appel *et al.* (E865 Collaboration), *Phys. Rev. Lett.* **85**, 2877 (2000)
- [21] R. Aaij *et al.* (LHCb Collaboration), *Phys. Rev. Lett.* **112**, 131802 (2014)
- [22] A. M. Sirunyan *et al.* (CMS Collaboration), *JHEP* **01**, 122 (2019)
- [23] M. Aaboud *et al.* (ATLAS Collaboration), *JHEP* **01**, 016 (2019)
- [24] P. Rubin *et al.* (CLEO Collaboration), *Phys. Rev. D* **82**, 092007 (2010)
- [25] M. Ablikim *et al.* (BESIII Collaboration), *Phys. Rev. D* **99**, 112002 (2019)
- [26] M. Ablikim *et al.* (BESIII Collaboration), *Nucl. Instrum. Meth. A* **614**, 345 (2010)
- [27] C. H. Yu *et al.*, *Proceedings of IPAC2016*, Busan, Korea, (2016)
- [28] M. Ablikim *et al.* (BESIII Collaboration), *Chin. Phys. C* **44**, 040001 (2020)
- [29] P. Cao *et al.*, *Nucl. Instrum. Meth. A* **953**, 163053 (2020)
- [30] S. Agostuneli *et al.* (GEANT4 Collaboration), *Nucl. Instrum. Meth. A* **506**, 250 (2003)
- [31] K. X. Huang, *et al.*, *Nucl. Sci. Tech.* **33**, 142 (2022)
- [32] S. Jadach, B. F. L. Ward, and Z. Was, *Comp. Phys. Commu.* **130**, 260 (2000)
- [33] S. Jadach, B. F. L. Ward, and Z. Was, *Phys. Rev. D* **63**, 113009 (2001)
- [34] D. J. Lange, *Nucl. Instrum. Meth. A* **462**, 152 (2001)
- [35] D. J. Lange, *Chin. Phys. C* **32**, 599 (2008)
- [36] R. L. Workman *et al.* (Particle Data Group), *Prog. Theor. Exp. Phys.* **2022**, 083C01 (2022)
- [37] J. C. Chen, G. S. Huang, X. R. Qi *et al.*, *Phys. Rev. D* **62**, 034003 (2000)
- [38] R. L. Yang, R. G. Ping, and H. Chen, *Chin. Phys. Lett.* **31**, 061301 (2014)
- [39] E. Richter-Was, *Phys. Lett. B* **303**, 163 (1993)
- [40] H. Albrecht *et al.* (ARGUS Collaboration), *Phys. Lett. B* **241**, 278 (1990)
- [41] Ryd A, Lange D, Kuznetsova N, *et al.*, *EvtGen: a Monte Carlo generator for B-physics*. *BAD* **522**, v6 (2005)
- [42] G. Punzi, arXiv: [2011.11770](#)
- [43] X. Y. Zhou, S. X. Du, G. Li *et al.*, *Comput. Phys. Commun.* **258**, 107540 (2021)
- [44] W. A. Rolke, A. M. Lopez, and J. Conrad, *Nucl. Instrum. Meth. A* **551**, 493 (2005)